JOURNAL OF GEOPHYSICAL RESEARCH, VOL. 91, NO. C1, PAGES 923–932, JANUARY 15, 1986

Measurement of the Ocean Wave-Radar Modulation Transfer Function at 4.3 GHz

J. SCHRÖTER AND F. FEINDT

Max-Planck-Institut für Meteorologie, Hamburg, Federal Republic of Germany

W. ALPERS

Fachbereich 1, Universität Bremen, Federal Republic of Germany

W. C. KELLER

Naval Research Laboratory, Washington, D. C.

Measurements of the ocean wave-radar modulation transfer function M at 4.3 GHz (C band) carried out in the North Sea are presented here. It was found that the values for M for C band lie within the same range as for X, L, and K_a bands. The measurements were made at incidence angles of 54° (HH and VV polarization) and 40° (VV polarization only). It was found that M decreases with increasing wind speed U and ocean wave frequency f. The phase of M was such that maximum backscatter occurs at the forward (leeward) face of the long ocean waves. For small dimensionless frequencies, $f^* = (fU)/g$, the modulus of M reaches values of up to 30. This indicates that there is a source of strong hydrodynamic modulation, most probably wind induced, that is as yet unexplained by existing theories.

1. INTRODUCTION

Microwave techniques for measuring ocean surface wave spectra have recently received considerable attention, since they can be applied from aircraft or satellites for monitoring sea state. Microwave instruments capable of performing such measurements include the real aperture imaging radar, the synthetic aperture imaging radar (SAR), and the two-frequency scatterometer and the short-pulse microwave spectrometer [see, e.g., *Alpers and Hasselmann*, 1978; *Johnson and Weissman*, 1984; *Jackson et al.*, 1985].

The measurement principle of all these instruments is based on the fact that long ocean waves modulate the radar cross section. In order to derive ocean wave spectra from data acquired by these microwave sensors, the ocean wave-radar modulation transfer function (MTF) must be known.

The ocean wave-radar MTF can, in principle, be measured by microwave scatterometers mounted on sea-based platforms. A cross-spectral analysis of the backscattered power from a small ocean patch and the ocean wave height or ocean wave slope yields the MTF [*Alpers and Jones*, 1978; *Wright et al.*, 1980]. The wave slope can be measured in situ, e.g., by a pitch-and-roll buoy, or by the radar itself by exploiting the information contained in the Doppler shift. The Doppler shift originates from the line-of-sight motion of the illuminated ocean patch and can be converted to wave slope [see, e.g., *Plant et al.*, 1983; *Feindt et al.*, 1986].

Extensive measurements of the ocean wave-radar MTF have been performed at 9.3 GHz (X band) and 1.5 GHz (L band) [*Plant et al.*, 1978, 1983; *Wright et al.*, 1980] but only a few at C band [*DeStaerke and Fontanel*, 1981]. With the advance in the work on the First European Remote Sensing Satellite (ERS-1), to be launched in 1990, which will carry a C band SAR for imaging ocean surface waves, there is a need for modulation experiments at C band. C band denotes the frequency band between 4.0 and 8.0 GHz.

In this paper we report about modulation experiments at 4.3 GHz that were carried out at the German North Sea Research Platform (Forschungsplattform Nordsee (FPN)) in 1981 from June 26 to July 1 and from December 2 to 14.

2. DEFINITION OF THE OCEAN WAVE-RADAR MODULATION TRANSFER FUNCTION

Let $\zeta(\mathbf{x}, t)$ be the ocean surface wave height function and $\sigma(\mathbf{x}, \vec{\mathbf{K}}, t)$ the radar backscattering cross section per unit surface area or normalized radar cross section (NRCS) in $\vec{\mathbf{K}}$ direction. A Fourier representation of these quantities reads

$$\zeta(\mathbf{x}, t) = \int [z(\mathbf{k})e^{i(\mathbf{kx}-\omega t)} + \text{c.c.}]\, d\mathbf{k} \tag{1}$$

$$\sigma(\mathbf{x}, \vec{\mathbf{K}}, t) = \sigma_0(\vec{\mathbf{K}}) + \int [\sigma(\mathbf{k}, \vec{\mathbf{K}})e^{i(\mathbf{kx}-\omega t)} + \text{c.c.}]\, d\mathbf{k} \tag{2}$$

Here $\mathbf{k}$ and ω denote the two-dimensional wave vector and angular frequency of the (large scale) ocean wave field, respectively, and $\vec{\mathbf{K}}$ the three-dimensional radar wave vector. The $z(\mathbf{k})$ and $\sigma(\mathbf{k}, \vec{\mathbf{K}})$ are complex random variables, and c.c. stands for complex conjugate. The $\sigma_0(\vec{\mathbf{K}})$ denotes the average radar backscattering cross section per unit surface area for a particular implied polarization. An ocean wave height-radar MTF can then be defined by

$$\frac{\sigma(\mathbf{k}, \vec{\mathbf{K}})}{\sigma_0(\vec{\mathbf{K}})} = R(\mathbf{k}, \vec{\mathbf{K}})z(\mathbf{k}) \tag{3}$$

$R(\mathbf{k}, \vec{\mathbf{K}})$ must be invariant with respect to rotations in the horizontal plane, which implies that R is only a function of $|\vec{\mathbf{K}}|$, $|\mathbf{k}|$, $\mathbf{k} \cdot \mathbf{K}$, and K_3 ($\mathbf{K}$ is the projection of $\vec{\mathbf{K}}$ onto the horizontal plane and K_3 the vertical component of $\vec{\mathbf{K}}$). An equivalent set of variables is the radar frequency $(c|\vec{\mathbf{K}}|)/(2\pi)$, where c is the speed of light, the ocean wave frequency $f = [g|\mathbf{k}| \tanh (|\mathbf{k}|D)]^{1/2}/(2\pi)$, where D is water depth, the azimuth angle $\varphi = \cos^{-1} [(\mathbf{k} \cdot \mathbf{K})(|\mathbf{k}|\,|\mathbf{K}|)^{-1}]$, and the incidence angle $\theta_i = \cos^{-1}$

Paper number 5C0740.
0148-0227/86/005C-0740$05.00

$K_3|\vec{\mathbf{K}}|^{-1}$). R may also be a function of environmental parameters, e.g., wind speed, air-sea temperature difference, sea surface temperature, or sea slick coverage.

The wave height spectrum in two-dimensional wave number space is defined by

$$\langle z^*(\mathbf{k})z(\mathbf{k}')\rangle = \tfrac{1}{2}\delta(\mathbf{k}-\mathbf{k}')G_\zeta(\mathbf{k}) \tag{4}$$

and the spectrum of the radar backscattering cross section $G_\sigma(\mathbf{k}, \vec{\mathbf{K}})$ by

$$\langle \sigma^*(\mathbf{k}, \vec{\mathbf{K}})\sigma(\mathbf{k}', \vec{\mathbf{K}})\rangle = \tfrac{1}{2}\delta(\mathbf{k}-\mathbf{k}')G_\sigma(\mathbf{k}, \vec{\mathbf{K}}) \tag{5}$$

Here $\langle\ \rangle$ denotes the ensemble average over the large-scale wave field and $\delta(\mathbf{k})$ the Dirac delta function. The complex conjugate of a function is denoted with an asterisk. Likewise, the cross spectrum $G_{\sigma,\zeta}(\mathbf{k}, \vec{\mathbf{K}})$ between radar cross section and wave height is defined by

$$\langle \sigma^*(\mathbf{k}, \vec{\mathbf{K}})z(\mathbf{k}')\rangle = \tfrac{1}{2}\delta(\mathbf{k}-\mathbf{k}')G_{\sigma,\zeta}(\mathbf{k}, \vec{\mathbf{K}}) \tag{6}$$

In terms of spectral quantities, the ocean wave height-radar MTF is then given by

$$R(\mathbf{k}, \vec{\mathbf{K}}) = \frac{1}{\sigma_0(\vec{\mathbf{K}})}\frac{G_{\sigma,\zeta}(\mathbf{k}, \vec{\mathbf{K}})}{G_\zeta(\mathbf{k})} \tag{7a}$$

$$R(\mathbf{k}, \vec{\mathbf{K}}) = \frac{1}{\sigma_0(\vec{\mathbf{K}})}\gamma_{\sigma,\zeta}(\mathbf{k}, \vec{\mathbf{K}})\left[\frac{G_\sigma(\mathbf{k}, \vec{\mathbf{K}})}{G_\zeta(\mathbf{k})}\right]^{1/2} \tag{7b}$$

where $\gamma_{\sigma,\zeta}$ denotes the coherence function between radar cross section and the wave height.

It should be stressed that the above description of the modulation of the radar backscattering by the long ocean waves is only valid when the process is linear. Measurements show that often the linear theory is adequate for describing the cross-section modulation. However, deviations from linearity seem to occur for high sea states. A measure of linearity is the coherence function. The closer $\gamma_{\sigma,\zeta}$ is to 1, the more linear is the process. When $\gamma_{\sigma,\zeta} = 1$,

$$\frac{1}{\sigma_0^2(\vec{\mathbf{K}})}G_\sigma(\mathbf{k}, \vec{\mathbf{K}}) = |R(\mathbf{k}, \vec{\mathbf{K}})|^2 G_\zeta(\mathbf{k}) \tag{8}$$

holds.

Other possible reasons for the coherence function $\gamma_{\sigma,\zeta}$ to be smaller than 1, apart from nonlinearity, are receiver noise and the presence of other modulation mechanisms that are not wave induced. While we can exclude receiver noise as a significant contribution to the signal $\sigma(t)$ in the measurements reported here, other modulation mechanisms, such as gustiness of the wind, might play an important role. Even if the modulation transfer function were perfectly known, the presence of such a modulation would make the retrieval of wave height from radar imagery difficult.

Sometimes it is convenient to define a dimensionless modulation transfer function $\mathbf{M}$ that relates the ocean wave slope spectrum $G_{\nabla\zeta}$ to the cross section spectrum G_σ:

$$\mathbf{M}(\mathbf{k}, \vec{\mathbf{K}}) = \frac{-i}{\sigma_0(\vec{\mathbf{K}})}G_{\sigma,\nabla\zeta}(\mathbf{k}, \vec{\mathbf{K}})G_{\nabla\zeta}^{-1}(\mathbf{k}) \tag{9}$$

where ∇ denotes the gradient in two-dimensional $\mathbf{x}$ space.

We have included a factor of $-i$ in (9) to make the phase of $\mathbf{M}$ compatible with the definitions of other MTF's, i.e., positive phase indicates the maximum of $\mathbf{M}$ occurs on the leeward side of the long ocean waves, and zero phase indicates wave crest. $\mathbf{M}(\mathbf{k}, \vec{\mathbf{K}})$ is related to $R(\mathbf{k}, \vec{\mathbf{K}})$ by (see (3))

$$R(\mathbf{k}, \vec{\mathbf{K}}) = \mathbf{k}\cdot\mathbf{M}(\mathbf{k}, \vec{\mathbf{K}}) \tag{10}$$

The ocean wave slope-radar cross-section MTF $\mathbf{M}$ reflects more the physics of the modulation than does R, since the cross-section modulation is primarily determined by wave slope. Note also that $\mathbf{M}$ is a dimensionless complex vector quantity.

Following *Wright et al.* [1980] and *Plant et al.* [1983], we shall present in this paper the experimental results from measurements in terms of dimensionless MTF's. However, the modulation transfer function $\mathbf{M}(\mathbf{k}, \vec{\mathbf{K}})$, which is a two-component vector in two-dimensional wave number space, is not measured directly in our experiment. This tower-based scatterometer experiment yields an MTF, which depends on only one variable, the ocean wave frequency f. In the experiment reported in this paper we measure a MTF between the radar cross section and the Doppler shift in look direction of the antenna. Evidently, the information contained in the Doppler shift does not suffice to specify the ocean wave field completely. Doppler measurements with one antenna yield only one-dimensional information of a two-dimensional wave field.

Thus in order to infer $\mathbf{M}(\mathbf{k}, \vec{\mathbf{K}})$ from such tower-based scatterometer experiments, one must

1. Perform measurements at different relative angles to the wave field.
2. Have additional information on the two-dimensional wave spectrum.
3. Use the dispersion relation for water waves in order to transform from frequency to wave number space.
4. Know the transfer function that relates Doppler shift to wave height.

In this paper we are only concerned with those cases where the dominant propagation direction of the ocean waves (as measured by eye) is in the look direction of the antenna, which in turn is pointed into the wind direction. As a consequence, our measurements yield only the component of $\mathbf{M}(\mathbf{k}, \vec{\mathbf{K}})$ in the direction of $\mathbf{k}$, which we denote $M(\mathbf{k}, \vec{\mathbf{K}})$, where M is a complex number, $|M|$ denotes its modulus, and ϕ_M describes the phase by which M leads the crest of the ocean wave, as conventionally written [e.g., *Keller and Wright*, 1975; *Reece*, 1978; *Alpers and Jones*, 1978; *Wright et al.*, 1980, and others].

3. Modulation Mechanisms

In the linear approximation the radar cross-section modulation by the long ocean waves can be considered as the superposition of three modulations: the tilt, the range, and the hydrodynamic modulation [*Keller and Wright*, 1976]. Thus the total nondimensional MTF can be written as

$$M = M_{\text{tilt}} + M_{\text{range}} + M_{\text{hydr}} \tag{11}$$

The tilt modulation is due to the purely geometric effect that Bragg-scattering waves are seen by the scatterometer at different local incidence angles depending on their location on the long wave profile. The tilt modulation transfer function M_{tilt} can be calculated in the two-scale wave model [*Wright*, 1978; *Valenzuela*, 1978]. Note that M_{tilt} is purely imaginary. Explicit formulas are given by *Alpers et al.* [1981]. The range modulation M_{range} describes the change of distance between radar and illuminated ocean patch [*Keller and Wright*, 1976]. In our measurements it is always smaller than 1. The hydrodynamic modulation describes the nonuniform distribution of the short waves with respect to the long ocean wave field. Such a nonuniform distribution may be caused by linear and nonlinear interactions between short and long waves, nonuniform generation of short ripples by the wind, or spontaneous generation of short waves by breaking or nearly breaking waves [*Alpers et al.*, 1981].

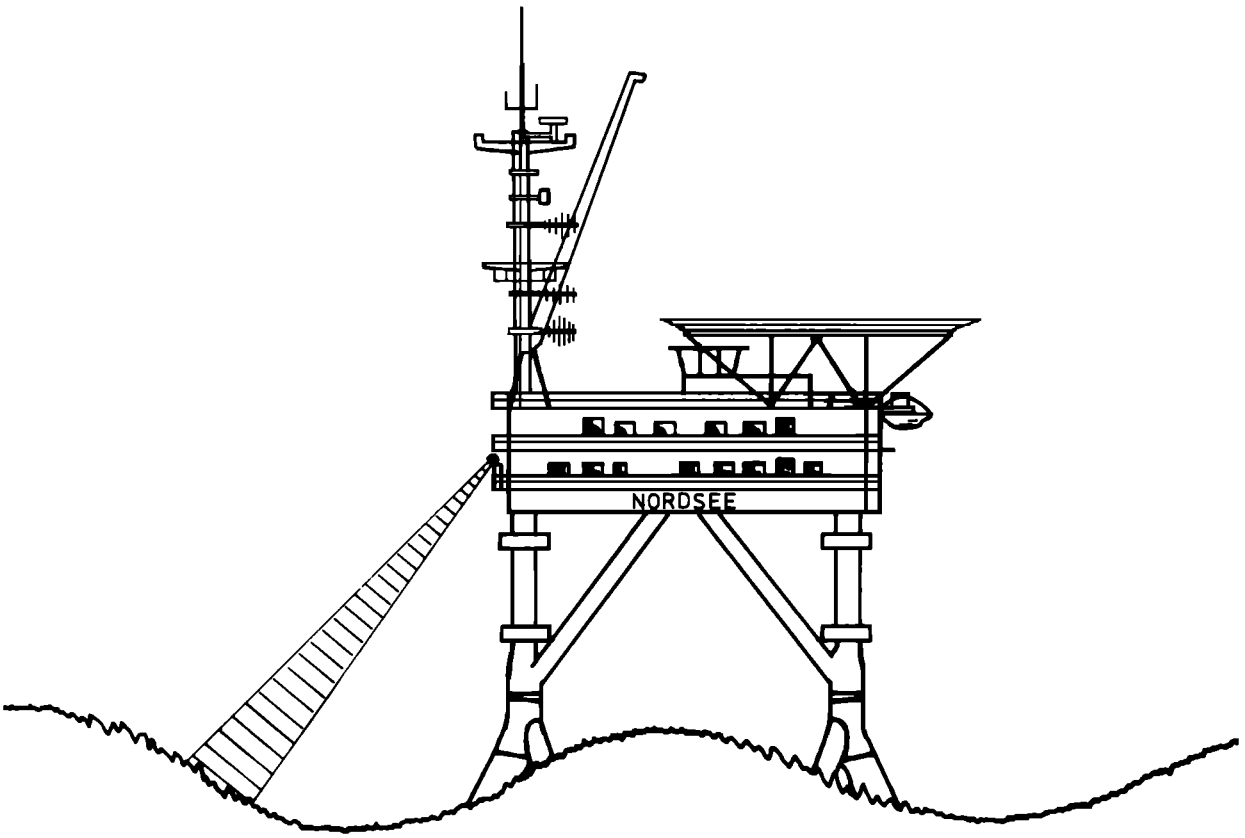

Fig. 1. Schematic view of the experiment at the research tower "Nordsee." The illuminated ocean patch is 2.3 × 1.6 m.

A satisfactory theory for describing the hydrodynamic modulation does not yet exist, although simplified theories based on the weak hydrodynamic interaction theory have been developed [*Longuet-Higgins and Stewart*, 1964; *Phillips*, 1977; *Keller and Wright*, 1975; *Alpers and Hasselmann*, 1978.].

4. THE EXPERIMENT

The experiment was performed in the North Sea between June 26 and July 1 and between December 2 and 14, 1981. The scatterometer was installed on the Forschungsplattform Nordsee (a German research platform) situated at 54° 42′00″N, 7°10′0″E, approximately 70 km west of the island of Sylt (West Germany). The water depth D at the site of the platform is 30 m.

Measurements were taken under a variety of wave and wind conditions. The significant wave height ($H_{1/3}$) varied from 0.2 to 3.5 m, and the wind speed measured at a height of 46 m on the platform varied from 3 to 16 m s^{-1}. Although the air-sea temperature difference ranged from 0.5°C to −5.6°C, it was between −2°C and −3°C for approximately 80% of the data reported here.

4.1. *The Instrument*

The scatterometer is a continuous wave (CW) system operating at 4.3 GHz (C band). Two separate antennas were used, a 76-cm shrouded parabolic antenna for transmission and a 137-cm parabolic antenna for reception. Both antennas were mounted on the railing of the platform at a height of 22.5 m above mean sea level (see Figure 1). At an incidence angle of 45°, the 6-dB footprint dimensions of the receiving antenna are $L_x = 2.3$ m in ground range direction and $L_y = 1.6$ m in azimuth direction. During a second measurement phase, the radar was changed to a pulsed system to increase the signal to noise ratio. This enabled us to measure successfully at HH polarization. For the pulsed system, the 137-cm antenna was used, for both transmitting and receiving. In order to adequately resolve the long ocean waves, the footprint should be smaller than one sixth of the ocean wavelength [*Keller and Wright*, 1976]. For our measurement geometry we were thus limited to ocean wave frequencies of less than 0.35 Hz.

The transmitter consists of a crystal-controlled oscillator with an output of 1 W. In this experiment the backscattered signal was beaten down to a variable offset frequency (most of the time, 340 Hz) such that the frequency excursions due to the motion of the water surface always resulted in positive frequencies. The Doppler spectrum of the backscattered signal was constantly monitored by a Hewlett-Packard HP 3582A spectral analyzer. The data were analog recorded on a Hewlett-Packard 3964 tape recorder running at $1\frac{7}{8}$ in. s.

4.2. *Data Analysis*

The tapes were digitized with a sampling frequency of 1 kHz. Given an offset frequency of 340 Hz, this means that positive Doppler shifts up to a frequency of 160 Hz, corresponding to a line-of-sight velocity of 5.6 m s^{-1}, could be analyzed. There were 128 values used to compute the "instantaneous" Doppler shift every 0.128 s. The spectrum was then smoothed by using a running average. From this smoothed spectrum the frequency of the spectral peak was determined. In order to increase the signal to noise ratio, only frequencies above 125 Hz were taken into account (equivalent to high-pass filtering).

The backscattered power P is obtained from the instantaneous Doppler spectrum by calculating the variance (integral

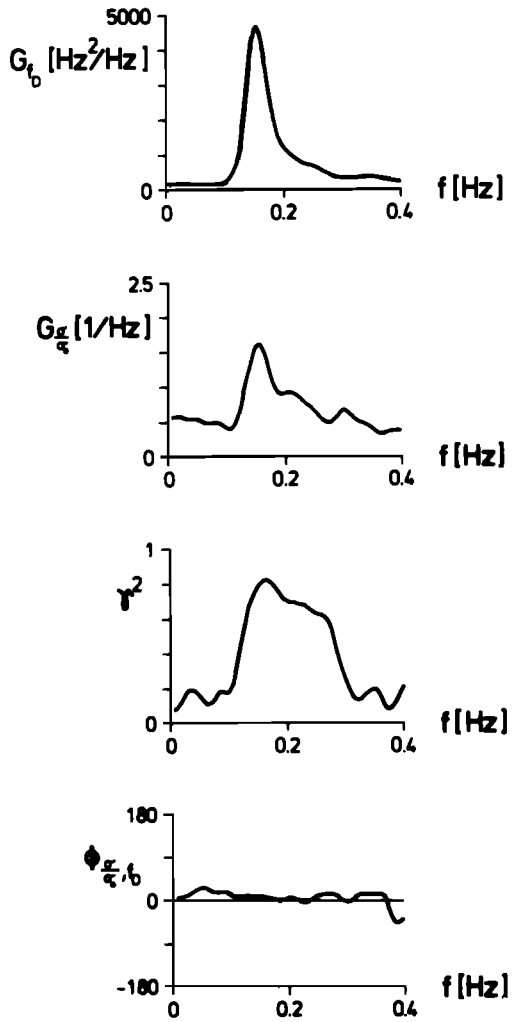

Fig. 2. (From top to bottom) (*a*) Power spectrum of the Doppler shift of the backscattered signal f_D, (*b*) power spectrum of the radar cross-section variation σ/σ_0, (*c*) square of coherence function γ^2, and (*d*) phase factor ϕ between σ/σ_0 and f_D. The data originate from measurements made on June 26, 1981, with VV polarization, 40° incidence angle, and an azimuth angle φ of 10° relative to the wind direction. The wind speed was 15.7 m s^{-1}.

of the spectrum). This variance is proportional to the radar cross section σ.

Thus two slow time series with data points every 0.128 s are created, one representing the instantaneous mean Doppler shift $f_D(t)$ in look direction of the antenna and the other the backscattered power $P(t)$. Since only relative variations of $P(t)$ enter into the calculation of the MTF, it is convenient to divide $P(t)$ by its average value P_0. Because of the proportionality between the backscattered power $P(t)$ and the radar cross section $\sigma(t)$, we have

$$\frac{P(t)}{P_0} = \frac{\sigma(t)}{\sigma_0} \tag{12}$$

The autospectra and cross spectra are calculated from these time series by using individual time records (chunks) of 132-s duration. Spectral averages are taken over 15 records, such that the total record length used for calculating spectral values totals 33 min. The final autospectra and cross spectra are smoothed by using a Hanning filter technique. The spectral resolution is thus reduced to 0.03 Hz, and the resulting equivalent degrees of freedom are increased to 120.

As an example, spectra of $f_D(t)$ and $\sigma(t)/\sigma_0$ as well as the square of the coherence function γ^2 and the phase factor ϕ between $G_{\sigma/\sigma_0}(f)$ and $G_{f_D}(f)$, as defined, e.g., by *Bendat and Piersol* [1966], are shown in Figure 2. As can be seen from this example, the normalized cross-section spectrum is always broader than the corresponding Doppler spectrum. This is an indication that $R(f)$ increases with f.

As the illuminated ocean patch is relatively long in range direction ($L_x = 2.3$ m) compared with the wavelength of the Bragg-scattering ocean ripple wave ($\lambda = 4.3$ cm), several small facets with individual radar cross sections and Doppler shifts contribute to the backscattered signal. In our analysis the Doppler f_D is identified as that of the dominant facet (i.e., with the largest radar cross section), while the Doppler information from the other facets, which manifests itself in sidebands of the instantaneous Doppler spectrum, is neglected.

The backscattered power of all facets is summed to give $\sigma(t)$. The contribution of the dominant facet is typically 3 dB higher than that of all the others combined. These other contributions cannot be regarded simply as noise, since their Doppler frequencies are highly correlated with that of the dominant facet. Therefore we can expect that the measured

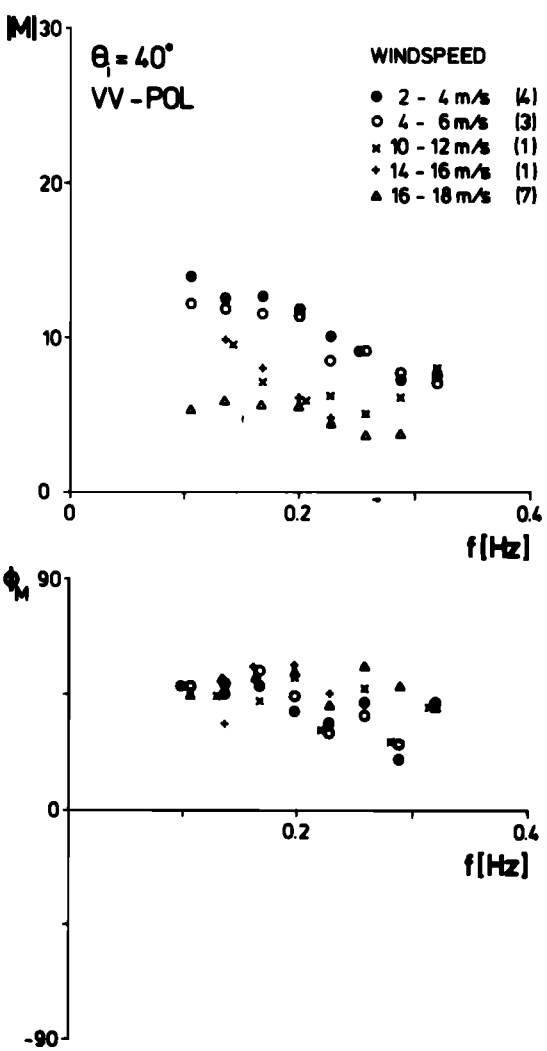

Fig. 3. (Top) Modulus and (bottom) phase of the dimensionless modulation function M versus ocean wave frequency for various wind speeds. The numbers in parentheses denote the number of events averaged. Measurements refer to VV polarization and 40° incidence angle.

coherence function between Doppler shift and backscattered power is smaller than 1.

In our analysis, we use only those spectral values for calculating M that lie in the frequency range 0.1 Hz $< f <$ 0.35 Hz and for which $\gamma^2 > 0.3$. With 120 degrees of freedom given, this means the modulus of the measured MTF lies between 0.50 and 1.66 times the true one (90% confidence limits and assuming the coherence function were true). A typical value for γ^2 is 0.5, with corresponding 90% confidence limits of 0.65 and 1.4. Confidence intervals for the phase of M are $\pm 17°$ for $\gamma^2 = 0.3$ and $\pm 11°$ for $\gamma^2 = 0.5$.

By correlating the series $f_D(t)$ and $\sigma(t)/\sigma_0$, we obtain cross spectra between the Doppler shift in look direction of the antenna and the normalized radar cross section in the same direction. From these we calculate the MTF M as a function of frequency (not wave number), as is conventionally done [*Keller and Wright*, 1975; *Alpers and Jones*, 1978; *Plant et al.*, 1978; *Wright et al.*, 1980]. The wave height spectrum $G_\zeta(f)$ is obtained from the spectrum of the Doppler shift $G_{f_D}(f)$ via [see *Hühnerfuss et al.*, 1981; *Plant et al.*, 1983; *Feindt et al.*, 1986]

$$G_{f_D}(f) = G_\zeta(f) 4|\vec{\mathbf{K}}|^2 f^2(|\mathbf{k}|)\left(\frac{\sin^2\theta_i \cos^2\varphi}{\tanh^2(|\mathbf{k}|D)} + \cos^2\theta_i\right) \tag{13}$$

Here φ is the angle between the wave propagation direction and the antenna azimuth direction. The relationship between

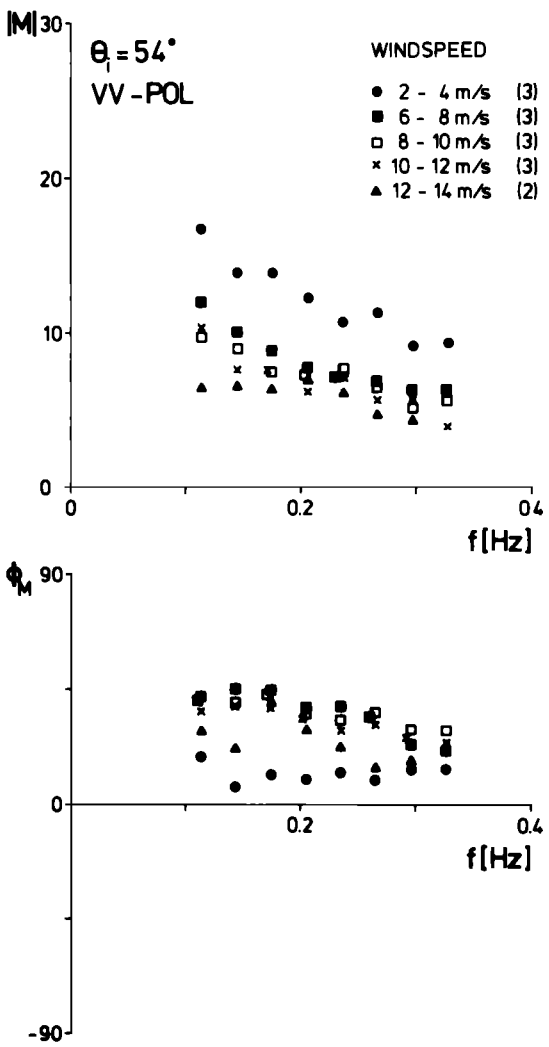

Fig. 4. Same as Figure 3 except that the incidence angle is 54°.

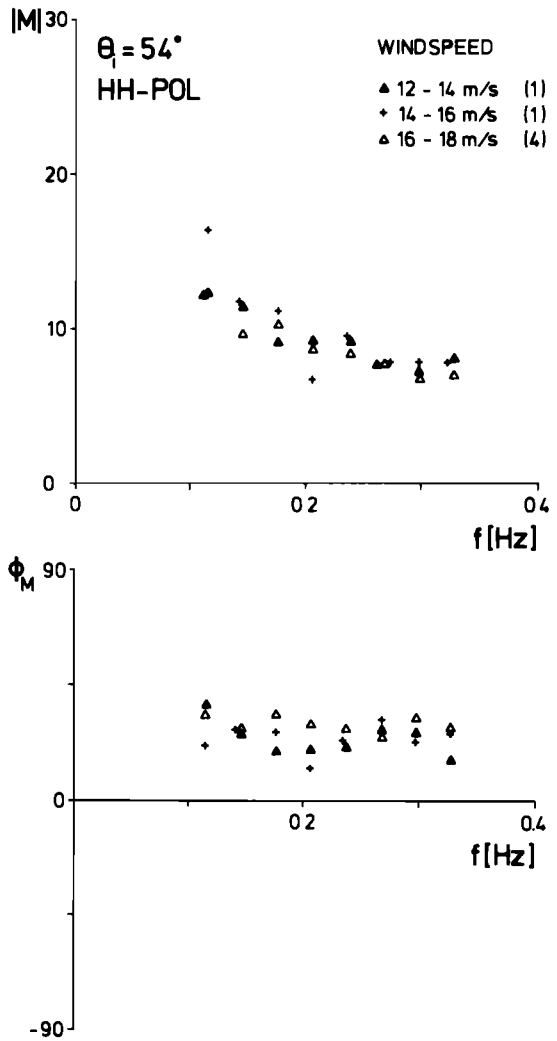

Fig. 5. Same as Figure 4 but for HH polarization ($\theta_i = 54°$).

the frequency f and the wave number $|\mathbf{k}|$ of an ocean wave traveling in water of depth D is given by the dispersion relation

$$f^2 = \frac{g}{4\pi^2}|\mathbf{k}| \tanh(|\mathbf{k}|D) \tag{14}$$

In calculating $G_\zeta(f)$, we assume that the wave field is unidirectional for the frequencies between 0.1 and 0.35 Hz. Since the relation between wave height and Doppler shift is linear, the coherence functions $\gamma_{\sigma,\zeta}$ and γ_{σ,f_D} are identical, and we can calculate $M(f)$ using (7), (10), (13), and (14).

In all, about 200 hours of data were recorded during the experiment. However, the data set was reduced considerably to ensure that only data of the highest quality were used to calculate M. We discarded all data for which any of the following criteria applied.

1. The spillover between transmitted and received signal was higher than −20 dB of the received signal (this applied to all HH measurements in the summer campaign).

2. The shape of the spectrum G_{σ/σ_0} was such that either values for frequencies below 0.05 Hz exceeded one half of the maximum value, or maxima were obtained for frequencies other than those of the dominant ocean waves.

3. Either the mean value or the variance of one of the time series $f_D(t)$ or $\sigma(t)$ could not be regarded as stationary during

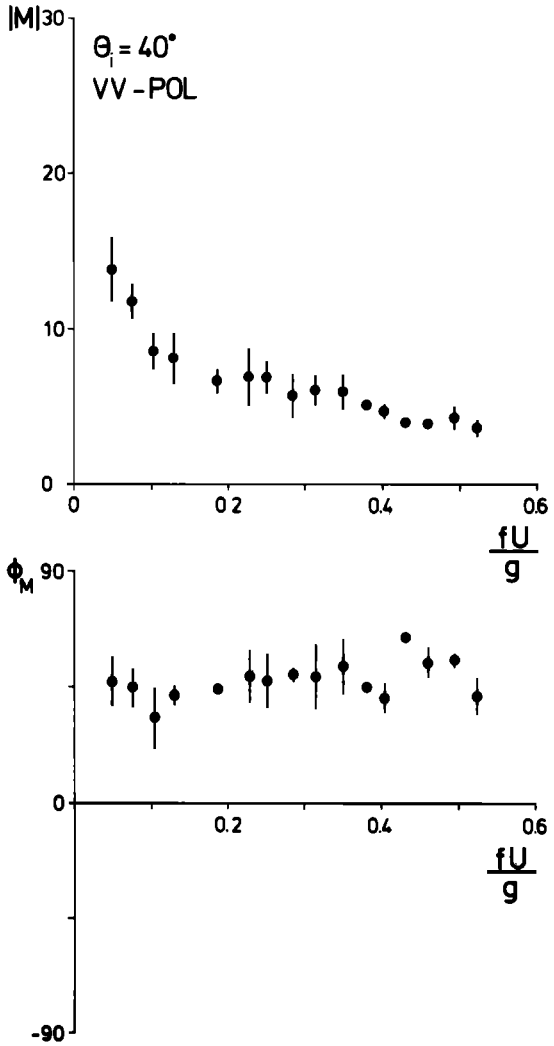

Fig. 6. (Top) Modulus and (bottom) phase of the dimensionless modulation transfer function as a function of the dimensionless frequency $f^* = (fU)/g$. Vertical bars denote two standard deviations of the measurements averaged for each frequency bin. Incidence angle θ_i is 40° and polarization is VV. This figure corresponds to Figure 3.

the measurement period of 33 min. We tested this using the reverse arrangement test, which is a very powerful test, with confidence limits of 5% and 95%, respectively [see *Bendat and Piersol*, 1966, p. 221].

4. The direction of the ocean waves could not be identified with sufficient accuracy or there were different wave systems present.

5. Results

The dependence of the ocean wave-radar MTF M on wind speed and ocean wave frequency is plotted in Figures 3–5. All measurements were taken under "upwind" conditions, meaning that wind and wave directions were approximately antiparallel to the horizontal direction of the radar antenna. Incidence angle and polarization of the radar waves are indicated in the figures. No data are available for HH polarization and 40° incidence angle. The number of events that were averaged in each wind speed interval are given in parentheses in Figures 3–5. Individual measurements of M show considerable scatter, which is slightly larger than the confidence limits of the measurements (see section 4.2). This indicates that environmental parameters other than those we have included in the analysis influence M. For instance, one candidate could be the air-sea temperature difference. Figures 3–5 show that the modulus of M decreases when the ocean wave frequency f and the wind speed U increases. The phase of M lies roughly between 10° and 60° on the forward face of the waves and shows no clear dependence on either f or U. Note that the main contribution to the measured M originates from the hydrodynamic modulation. For the parameters encountered during the experiment, the range modulation is always less than 1. Furthermore, the theoretical values for the tilt modulation $|M_{\text{tilt}}|$ are [*Alpers et al.*, 1981] 3.7 for $\theta_i = 40°$, VV polarization (Figure 3); 2.6 for $\theta_i = 54°$, VV polarization (Figure 4); and 7.9 for $\theta_i = 54°$, HH polarization (Figure 5).

In the calculation of M_{tilt} we have assumed a wave spectrum $G_\zeta(\mathbf{k})$ that is proportional to $|\mathbf{k}|^{-4}$ in the region of the Bragg-scattering ripple waves. Under our measurement conditions (upwind), the phase of the tilt modulation is 90° downwave (leeward) from the long wave crest.

As M is a dimensionless quantity, it should be dependent only on dimensionless quantities. The appropriate choice for such a quantity is the dimensionless frequency $f^* = (fU)/g$, where g is the acceleration of gravity.

The dependence of M on this dimensionless frequency f^* corresponding to Figures 3–5 is plotted in Figures 6–8. Verti-

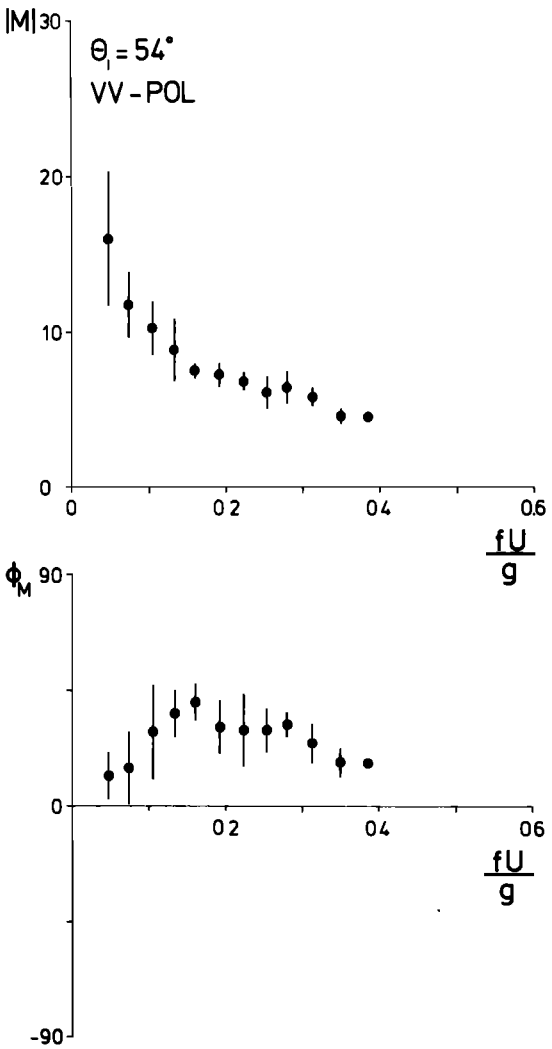

Fig. 7. Same as Figure 6 except that the incidence angle is 54° (corresponding to Figure 4).

cal bars indicate 2 standard deviations of the values averaged in every frequency interval. In some cases this bar is smaller than the solid circle, which indicates the mean value. Generally, the scatter in the measured values is approximately the same or slightly smaller than that for a fixed wind speed or fixed frequency interval. Thus the dimensionless frequency is the appropriate independent parameter to be used for exhibiting the dependence of M on both wind speed and ocean wave frequency. Note that for a fully developed wind sea, the spectral peak of the ocean waves has the value 0.14 for f^*. Since the wind speed was measured at a height of 46 m and not at 19.5 m, the level for which the value of 0.14 is applicable [*Pierson and Moskowitz*, 1964], a value of approximately 0.15 is the frequency f^* of the peak of the wave spectrum for a fully developed sea to be used in Figures 6–8. There is, however, no indication that the modulation observed for swell ($f^* < 0.15$) is fundamentally different from the modulation for wind sea ($f^* > 0.15$).

The decrease of M with increasing frequency cannot simply be explained by the ratio of the wavelength λ of the long ocean waves to the length L_x of the radar footprint. This ratio is proportional to $|\mathbf{k}|^{-1}$ and thus to f^{-2} (deep water assumed). We would predict therefore a decrease of M proportional to f^{-2}. The falloff of the measured M with f for fixed wind speed lies approximately between $f^{-1/2}$ and f^{-1}, which contradicts the prediction made above. Only for high frequencies, where L_x becomes comparable to λ, we expect such a dependence, e.g., for L_x equal to the ocean wavelength, M should be 0.

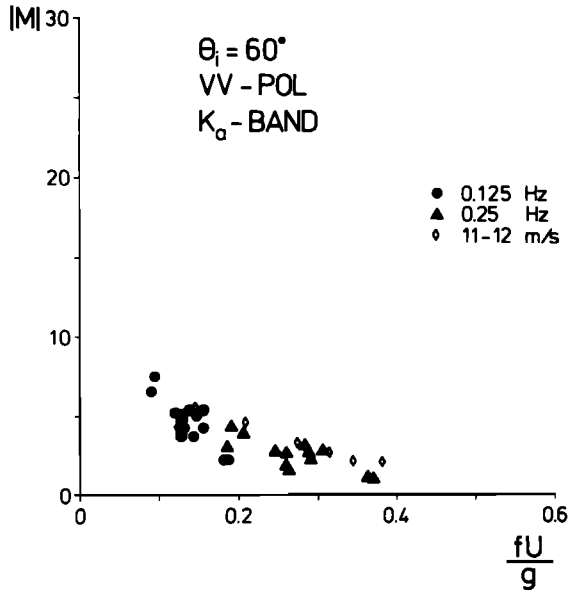

Fig. 9. Modulus of the dimensionless K_a band (35 GHz) modulation transfer function at VV polarization and 60° incidence angle as a function of the dimensionless frequency f^*. The data are taken from *Feindt et al.* [1986].

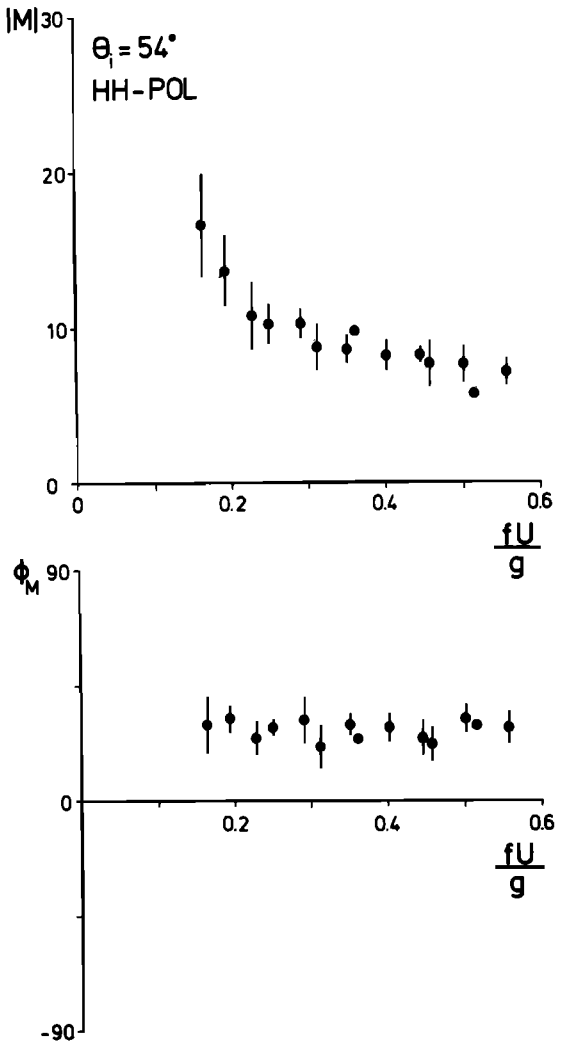

Fig. 8. Same as Figure 7 but for HH polarization (corresponding to Figure 5).

Another possible explanation for a dependence of M on f is the effect of an angular spreading function for the ocean waves that depends on f. However, this effect is small and cannot account for differences, in M, of a factor of 5 and above. This is shown in Appendix A.

6. Comparison With Modulation Experiments at Other Radar Frequencies

The modulus of the C band (4.3 GHz) MTF differs very little from the modulus of the MTF at K_a band (35 GHz) [*Feindt et al.*, 1986], at X band (9.35 GHz) [*Alpers and Jones*, 1978; *Wright et al.*, 1980; *Plant et al.*, 1983; *Keller et al.*, 1985], or at L band (1.56 GHz) [*Wright et al.*, 1980; *Plant et al.*, 1983]. High values occur primarily at low frequencies and low wind speeds. For these cases, the weak hydrodynamic interaction theory [*Keller and Wright*, 1975; *Alpers and Hasselmann*, 1978] is not adequate for describing the measured values of M_{hydr}. Note that the increase of $|M|$ with decreasing frequency is solely due to the factor $|\mathbf{k}|^{-1}$ in the definition of M (R increases slightly with frequency). Large values of $|M|$ at low frequencies ($f < 0.15$ Hz) are equivalent to small values for R, and thus the linear perturbation expansion (3) is still applicable in this frequency range.

For comparison, the dependence of $|M|$ on the dimensionless frequency is plotted in Figures 9–11 also for K_a band (35 GHz) and X band (9.35 GHz). Data for K_a band are taken from *Feindt et al.* [1985], for X band from *Wright et al.* [1980] ("West Coast Experiment"), and from *Plant et al.* [1983] ("MARSEN"). No comparison is made for L band (1.56 GHz), since the modulation at this radar frequency seems to be either independent of the wind speed (MARSEN) [*Plant et al.*, 1983] or even slightly increasing with wind speed (West Coast Experiment) [*Wright et al.*, 1980].

We cannot exclude the possibility that this is an instrumen-

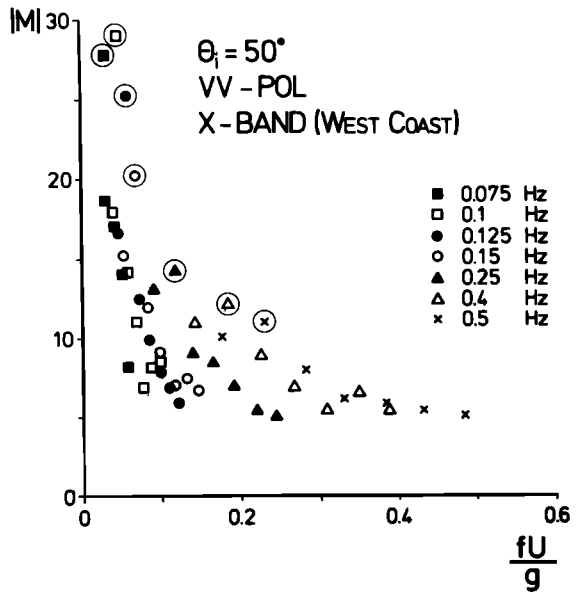

Fig. 10. Same as Figure 9 but for X band (9.35 GHz) and 50° incidence angle. Values are taken from *Wright et al.* [1980] West Coast Experiment. The circled values are for a wind speed of 4–5 m s^{-1}, where unusually high modulation was encountered.

tal effect, because the illuminated ocean patch was located in both experiments very close to the platform. In this case platform-induced disturbances of the wind and wave field could have had a large effect on the measurements. As the dependence of the phase of M on frequency is contradictory for X band in the two experiments mentioned above (West Coast and MARSEN), we have refrained from plotting the phase as a function of the dimensionless frequency. Values of $|M|$ for K_a band are generally smaller than those for C band. Note that the tilt modulation for K_a band is also slightly smaller than for C band ($M_{tilt} = 1.5$ for K_a band at $\theta_i = 60°$). For the West Coast Experiment, $|M|$ at X band is practically identical to what we measure at C band, if we disregard the exceptionally high values encountered at a wind speed of 4–5 m s^{-1} (circled data points in Figure 10). These high modulations are as yet unexplained. Values of $|M|$ at X band measured during MARSEN are somewhat smaller than those measured during the West Coast Experiment (Figure 11).

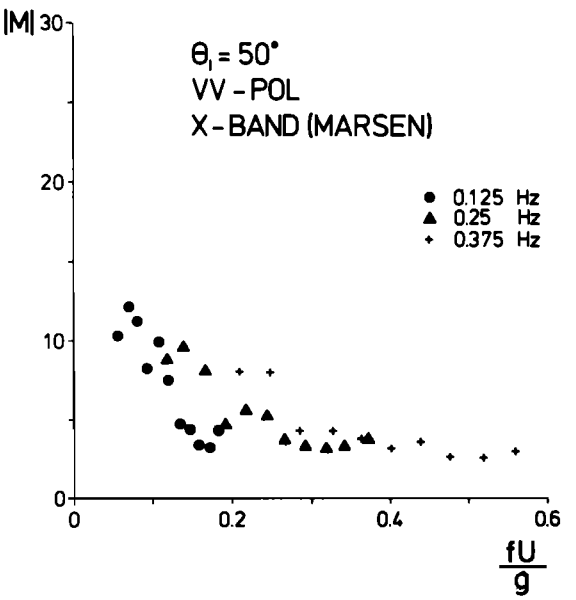

Fig. 11. Same as Figure 10 from measurements during MARSEN. The data are from *Plant et al.* [1983].

Since the definition of the modulation transfer function that was used to calculate M at X band is slightly different from our definition of M [*Wright et al.*, 1980; *Plant et al.*, 1983], values of $|M|$ for X band have to be divided by tanh ($|\mathbf{k}|D$) in order to make them compatible with our data (see Appendix B). This correction is small for the MARSEN experiment, but for the West Coast Experiment, values for low frequencies increase appreciably. Thus we conclude that the C band dimensionless MTF does not differ significantly from the X band dimensionless MTF.

7. Conclusions

The dimensionless modulation transfer function M measured at C band (4.3 GHz) under upwind conditions depends on the nondimensional frequency $f^* = (fU)/g$. For small dimensionless frequencies ($f^* < 0.05$), $|M|$ can be as large as 30, while for high frequencies ($f^* > 0.4$), $|M|$ is of the order of the tilt MTF M_{tilt}. At L band (1.56 GHz), $|M|$ has the same order of magnitude, but no clear dependence on wind speed is observed. At X band (9.35 GHz) and K_a band (35 GHz) the dependence of $|M|$ on f^* is similar to that for C band. This dependence cannot be explained by tilt and the weak interaction hydrodynamic modulation [*Keller and Wright*, 1975; *Alpers and Hasselmann*, 1978]. Furthermore, we also exclude instrumental effects as being a cause of the dependence of $|M|$ on f^*, since this dependence has been measured at different microwave frequencies, by different instruments, and under different environmental conditions. For explaining this frequency dependence, we can also exclude effects that are due to the ratio of the footprint size to the long ocean wavelength or to erroneous assumptions about the angular spread of the ocean wave spectrum. These effects are too small, as has been shown above. Thus we can conclude that there exists a hydrodynamic modulation for ocean waves with wavelength of 4 cm and below that depends on the dimensionless frequency f^*. C band is the lowest microwave frequency for which this observation holds.

8. Appendix A: Influence of the Angular Spreading Function for Ocean Waves on the Frequency Dependence of the MTF

We have assumed a unidirectional azimuthal distribution for the long waves in the calculation of the wave height spectrum via (13). This will lead to an underestimation of $G_\zeta(f)$, when the assumption is violated. If the azimuthal dependence of the MTF $M(f)$ is stronger than the azimuthal dependence of the spectrum of the Doppler shift $G_{f_D}(f)$ (13), then the calculated $M(f)$ will be underestimated too.

This underestimation of $M(f)$ depends on the shape of the spreading function, which in turn is a function of frequency. Thus the measured frequency dependence of $M(f)$ can, in part, be explained with an erroneous assumption about a frequency dependent spreading function for ocean waves.

Let us first consider the estimation of the wave-height spectrum via the use of (13). Since the measurements are made in the time domain, the spectra are in the frequency domain. Let $G_\zeta(f)$ be the one-dimensional wave height spectrum, integrated over all azimuth angles φ, as it would be measured by a wave staff. The angular dependence of the waves is described

by a spreading function $S(f, \varphi)$. S is normalized such that

$$\int_{-\pi}^{\pi} S(f, \varphi)\, d\varphi = 1$$

for all f. As the Doppler spectrum $G_{f_D}(f)$ depends on the azimuth angle φ (13), so does our estimate of $G_\zeta(f)$. Let us assume for simplicity an incidence angle $\theta_i = 45°$ and deep water (i.e., $\tanh(|\mathbf{k}|D) = 1$).

Then

$$G_\zeta^e(f) = G_\zeta^t(f) \int_{-\pi}^{\pi} S(f, \varphi)(\sin^2\theta_i \cos^2\varphi + \cos^2\theta_i)\, d\varphi$$

$$= G_\zeta^t(f)[0.5 + 0.5 \int_{-\pi}^{\pi} S(f, \varphi) \cos^2\varphi\, d\varphi] \quad \text{(A1)}$$

where superscripts e and t stand for "estimated" and "true," respectively.

The ratio $\beta = G_\zeta^e(f)/G_\zeta^t(f)$ depends on the spreading function S such that if S is a delta function at φ_0, then $\beta = (1 + \cos^2\varphi_0)/2$ (so if $\varphi_0 = 0$, i.e., it coincides with the radar look direction, then $\beta = 1$). For a spreading function $S(f, \varphi)$ that is isotropic, we obtain $\beta = 0.75$, and for $S(f, \varphi)$ proportional to $\cos^2\varphi$, then $\beta = 0.875$.

Let us write the dependence of the true MTF on azimuth direction as a product:

$$|M^t(f, \varphi)| = |M^t(f, \varphi = 0)| \cdot |M^t(\varphi)| \quad \text{(A2)}$$

Note that the function $|M^t(\varphi)|$ is not normalized:

$$\int_{-\pi}^{\pi} |M^t(\varphi)|\, d\varphi \neq 1 \quad \text{(A3)}$$

The part of $\sigma(f)$ that is coherent with the wave field can then be written as

$$[\sigma_{\text{coh}}(f)]^2 = \int_{-\pi}^{\pi} |M^t(f, \varphi = 0)|^2\, |M^t(\varphi)|^2 G_\zeta^t(f) S(f, \varphi)\, d\varphi$$

$$= |M^t(f, \varphi = 0)|^2 G_\zeta^t(f) \int_{-\pi}^{\pi} |M^t(\varphi)|^2 S(f, \varphi)\, d\varphi \quad \text{(A4)}$$

Since $[\sigma_{\text{coh}}(f)]^2$ is a quantity that we measure with the radar, we can express it as

$$[\sigma_{\text{coh}}(f)]^2 = |M^e(f, \varphi = 0)|^2 G_\zeta^e(f) \quad \text{(A5)}$$

Combined with (A3), we obtain

$$\frac{|M^e(f, \varphi = 0)|^2}{|M^t(f, \varphi = 0)|^2} = \frac{G_\zeta^t(f)}{G_\zeta^e(f)} \int_{-\pi}^{\pi} [M^t(\varphi)]^2 S(f, \varphi)\, d\varphi$$

$$= \beta^{-1} \int_{-\pi}^{\pi} [M^t(\varphi)]^2 S(f, \varphi)\, d\varphi \quad \text{(A6)}$$

Thus the smaller the right-hand side of (A6) is, the smaller is our estimate $|M^e(f, \varphi = 0)|$. If the true MTF $|M^t(f, \varphi = 0)|$ were not dependent on f, then the only dependence of $|M^e(f, \varphi = 0)|$ on f would be due to a combination of a strongly angular dependent $|M^t(\varphi)|$ and a spreading function S that is sharply peaked at low frequencies and is very broad at high frequencies. Let us assume $|M^t(\varphi)| = \cos^2\varphi$. This assumption is conservative, since, e.g., M_{tilt} is proportional to $\cos\varphi$. Also, $|M^t(\varphi = 90°)|$ is not zero [*Alpers et al.*, 1981; *Plant et al.*, 1983]. We will get the strongest frequency dependence of M if, for two given frequencies f_1 and f_2, S were proportional to a delta function and isotropic in the half space from $-\pi/2$ to $\pi/2$, respectively. For f_1 we obtain

$$|M^e(f_1, \varphi = 0)| = |M^t(f_1, \varphi = 0)| \quad \text{(A7)}$$

while for f_2 we obtain

$$|M^e(f_2, \varphi = 0)| = 2^{-1/2}\, |M^t(f_2, \varphi = 0)| \quad \text{(A8)}$$

Thus we have shown that the violation of the assumption we made in the calculation of $G_\zeta^t(f)$ (unidirectional wavefield) leads to an underestimation of the MTF for frequencies where the angular spread of the ocean waves is broad. However, the error is small and cannot account for the strong frequency dependence of M that is measured.

9. Appendix B: Relationship Between Differently Defined MTF's

Wright et al. [1980] and *Plant et al.* [1983] have conventionally defined the MTF in terms of the cross spectrum between the backscattered power P and the horizontal component of the orbital velocity u in the direction of wave propagation. Their definition of the modulation transfer function is

$$m = \frac{C_{ph}}{P_0} \frac{G_{P,u}}{G_u} = \frac{C_{ph}}{P_0} \gamma_{P,u} \left[\frac{G_P}{G_u}\right]^{1/2} \quad \text{(B1)}$$

where $G_{P,u}$ denotes the cross spectrum between P and u, G_u and G_P the power spectra of u and P, respectively, $\gamma_{P,u}$ the coherence function, C_{ph} the phase speed of the ocean waves, and P_0 the average backscattered power. G_u and the wave height spectrum G_ζ are related by

$$G_u(\omega) = \omega^2 \tanh^{-2}(|\mathbf{k}|D) G_\zeta(\omega) \quad \text{(B2)}$$

where $\mathbf{k}$ is the wave number and D the water depth.

We obtain after inserting (B2) into (B1)

$$m = \frac{C_{ph}}{P_0} \frac{\tanh(|\mathbf{k}|D)}{\omega} \gamma_{P,\zeta} \left[\frac{G_P}{G_\zeta}\right]^{1/2} \quad \text{(B3)}$$

since

$$C_{ph} = \frac{\omega}{|\mathbf{k}|} \quad \text{(B4)}$$

and

$$\frac{G_P}{P_0^2} = \frac{G_\sigma}{\sigma_0^2} = G_{\sigma_0/\sigma} \quad \text{(B5)}$$

we can rewrite (B3)

$$m = |\mathbf{k}|^{-1} \gamma_{P,\zeta} [G_{\sigma/\sigma_0}/G_\zeta]^{1/2} \tanh(|\mathbf{k}|D) \quad \text{(B6)}$$

A comparison of (7) and (10) with (B6) yields

$$|m| = |M| \tanh(|\mathbf{k}|D) \quad \text{(B7)}$$

Thus for deep water ($\tanh(|\mathbf{k}|D) = 1$) the two definitions are

TABLE B1. Values for $\tanh(|\mathbf{k}|D)$

West Coast Experiment (D = 18 m)		MARSEN (D = 30 m)	
f	$\tanh(\|\mathbf{k}\|D)$	f	$\tanh(\|\mathbf{k}\|D)$
0.075	0.60	0.125	0.96
0.100	0.75	≥0.250	1.00
0.125	0.87		
0.150	0.93		
≥0.2	1.00		

The definitions of the phase of the MTF's are identical.

identical. For shallower water, Wright et al. and Plant et al. will report a smaller modulation transfer function than this report does. Table B1 gives values for tanh ($|\mathbf{k}|D$) corresponding to frequencies that are relevant for this paper.

Acknowledgments. We thank the crew of the Forschungsplattform Nordsee for their help during the measurement campaigns. Special thanks go to Norman Smith of the University of Cambridge, U.K., for making his wave height and wave direction estimates available to us. This work was supported in part by the Bundesministerium für Forschung und Technologie and by the Deutsche Forschungsgemeinschaft.

REFERENCES

Alpers, W., and K. Hasselmann, The two frequency microwave technique for measuring ocean-wave spectra from an airplane or satellite, *Boundary Layer Meteorol., 13*, 215–230, 1978.

Alpers, W., and W. L. Jones, The modulation of the radar backscattering cross-section by long ocean waves, 12th International Symposium on Remote Sensing of Environments, pp. 1579–1608, Environ. Res. Inst. of Mich., 1978.

Alpers, W., D. B. Ross, and C. L. Rufenach, On the detectability of ocean surface waves by real and synthetic aperture radar, *J. Geophys. Res., 86*, 6481–6498, 1981.

Bendat, J. S., and A. G. Piersol, *Measurement and Analysis of Random Data*, John Wiley, New York, 1966.

DeStaerke, D., and A. Fontanel, Study of the modulation function by correlation in time and frequency domain of wave heights and microwave signal, paper presented at the Symposium on Wave Dynamics and Radio Probing of the Ocean Surface, Interunion Comm. on Radar Meteorol., Miami Beach, Fla., May 13–20, 1981.

Feindt, F., J. Schröter, and W. Alpers, Measurements of the ocean wave-radar modulation transfer function at 35 GHz (K_a band) from a sea-based platform in the North Sea, *J. Geophys. Res.*, in press, 1986.

Hühnerfuss, H., W. Alpers, W. L. Jones, P. A. Lange, and K. Richter, The damping of ocean surface waves by a monomolecular film measured by wave staffs and microwave radars, *J. Geophys. Res., 86*, 429–438, 1981.

Jackson, F. C., W. T. Walton, and P. L. Baker, Aircraft and satellite measurements of ocean wave directional spectra using scanning-beam microwave radars, *J. Geophys. Res., 90*, 975–986, 1985.

Johnson, J. W., and D. E. Weissman, Two-frequency microwave resonance measurements from an aircraft: A quantitative estimate of the directional ocean surface spectrum, *Radio Sci., 19*, 841–854, 1984.

Keller, W. C., and J. W. Wright, Microwave scattering and the straining of wind-generated waves, *Radio Sci., 10*, 139–147, 1975.

Keller, W. C., and J. W. Wright, Modulation of microwave backscatter by gravity waves in a wave tank, *NRL Rep. 7968*, Nav. Res. Lab., Washington, D. C., 1976.

Keller, W. C., W. J. Plant, and D. E. Weissman, The dependence of X band microwave sea return on atmospheric stability and sea state, *J. Geophys. Res., 90*, 1019–1029, 1985.

Longuet-Higgins, M. S., and R. W. Stewart, Radiation stresses in water waves: A physical discussion with applications, *Deep Sea Res., 11*, 529–562, 1964.

Phillips, O. M., *The Dynamics of the Upper Ocean*, 2nd ed., Cambridge University Press, New York, 1977.

Pierson, W. J., Jr., and L. Moskowitz, A proposed spectral form for fully developed wind seas based on the similarity theory of S. A. Kitaigorodskii, *J. Geophys. Res., 69*, 5181–5190, 1964.

Plant, W. J., W. C. Keller, and J. W. Wright, Modulation of coherent microwave backscatter by shoaling waves, *J. Geophys. Res., 83*, 1347–1352, 1978.

Plant, W. J., W. C. Keller, and A. Cross, Parametric dependence of ocean wave-radar modulation transfer functions, *J. Geophys. Res., 88*, 9747–9756, 1983.

Reece, A. M., Jr., Modulation of short waves by long waves, *Boundary Layer Meteorol., 13*, 203–214, 1978.

Valenzuela, G. R., Theories for the interaction of electromagnetic and ocean waves—A review, *Boundary Layer Meteorol., 13*, 61–85, 1978.

Wright, J. W., Detection of ocean waves by microwave radar: The modulation of short gravity-capillary waves, *Boundary Layer Meteorol., 13*, 87–105, 1978.

Wright, J. W., W. J. Plant, W. C. Keller, and W. L. Jones, Ocean wave-radar modulation transfer functions from the West Coast Experiment, *J. Geophys. Res., 85*, 4957–4966, 1980.

W. Alpers, Fachbereich 1 (Physik/Elektrotechnik), Universität Bremen, 2800 Bremen 33, Federal Republic of Germany.

F. Feindt and J. Schröter, Max-Planck-Institut für Meteorologie, Bundesstrasse 55, 2000 Hamburg 13, Federal Republic of Germany.

W. C. Keller, Naval Research Laboratory, Washington, DC 20375.

(Received April 16, 1985;
accepted May 20, 1985.)